PCCP

Cite this: *Phys. Chem. Chem. Phys.*, 2011, **13**, 21126–21131

www.rsc.org/pccp

PAPER

Titanium-decorated graphene oxide for carbon monoxide capture and separation†

Lu Wang,[ab] Jijun Zhao,*[ab] Lili Wang,[ab] Tianyin Yan,[c] Yi-Yang Sun[d] and Shengbai B. Zhang[d]

Received 1st June 2011, Accepted 6th October 2011
DOI: 10.1039/c1cp21778j

We propose titanium-decorated graphene oxide (Ti–GO) as an ideal sorbent for carbon monoxide (CO) capture and separation from gas mixtures. Based on first-principles calculations, Ti–GO exhibits a large binding energy of $\sim$70 kJ mol^{-1} for CO molecules, while the binding energies for other gases, such as N_2, CO_2, and CH_4, are significantly smaller. The gas adsorption properties of Ti–GO are independent of the local GO structures once Ti atoms are anchored by the oxygen-containing groups on the GO surface. The strong interaction between CO molecule and Ti is a result of dative bonding, *i.e.*, hybridization between an empty d orbital of Ti and an occupied p orbital of CO. Adsorption isotherms from grand canonical Monte Carlo simulations clearly demonstrate the strong selectivity of Ti–GO for CO adsorption in a mixture with other gas.

1. Introduction

Effective capture and separation of carbon monoxide (CO) is a crucial issue in the energy and environmental science. Release of industrial and vehicle exhaust gases into the atmosphere is one of the major sources of current environmental problems. Among the exhaust gases, CO is highly toxic to man.[1] From the aspect of energy science, CO is well known to be poisonous to some important catalysts for energy applications. For example, a small amount of CO contained in the hydrogen stream after the water–gas shift reactor can poison the platinum anode used in a polymer electrolyte membrane fuel cell.[2,3] Removal of CO from CO_2-rich mixtures is also an important step in the production of hydrogen from biomass.[4]

Among the possible solutions of CO removal[3] (such as selective diffusion of H_2 through the membrane, selective methanation, preferential oxidation), physical/chemical adsorption using appropriate sorbents offers a cost-effective and eco-friendly option.[5] Successfully finding an ideal sorbent for CO capture and separation is thus of great importance. To be an effective sorbent for large-scale industrial productions and applications, several criteria must be satisfied, such as permanent porosity with light mass, large surface area, low cost and easy to synthesize, favorable thermodynamics, fast kinetics, reversible capture and release.

Zeolites, with their uniform and tunable pores, have played a major role in the development of adsorption technology and have been widely used in industrial separation.[6] It was shown that the gas adsorption properties of zeolites depend on their framework composition and the unsaturated metal cations.[5–11] For example, Pillai *et al.* studied the CO, CH_4 and N_2 sorption in the alkali metal ion exchanged zeolite-X and found that the adsorbed molecules are mainly located at the open metal cation sites.[8] In addition to zeolites, other porous materials like activated carbon[12–16] and molecular sieve[17–19] can also be used for CO separation.

In recent years, owing to the exceptionally high surface area and permanent porosity, significant attentions have turned toward the use of nanoporous materials like metal organic frameworks (MOFs)[20–25] and zeolitic imidazole frameworks (ZIFs)[26,27] for gas separation. For example, Valenzano *et al.* investigated adsorption of CO, N_2 and CO_2 on Mg-MOF-74 by combining experimental infrared spectroscopy with *ab initio* calculations,[23] and the adsorption enthalpies from high to low were CO_2, CO and N_2, respectively. Yoon *et al.* demonstrated that the strength of CO adsorption on the MOF with coordinatively unsaturated sites can be enhanced by a controlled reduction of MIL-100(Fe), *i.e.*, a crystalline three-dimensional iron (III) trimesate.[24]

As a rising superstar in material science and nanoscience, graphene holds promise in the applications of many fields and has been intensively studied.[28,29] In addition to the pristine graphene, graphite/graphene oxide (GO) has recently attracted resurgent interests,[30–32] since it can be easily synthesized at low

[a] *Key Laboratory of Materials Modification by Laser, Ion and Electron Beams (Dalian University of Technology), Ministry of Education, Dalian 116024, China*
[b] *College of Advanced Science and Technology, Dalian University of Technology, 116024, China. E-mail: zhaojj@dlut.edu.cn*
[c] *Institute of New Energy Material Chemistry, Nankai University, Tianjin 300071, China*
[d] *Department of Physics, Applied Physics, and Astronomy, Rensselaer Polytechnic Institute, Troy, NY 12180, USA*
† Electronic supplementary information (ESI) available. See DOI: 10.1039/c1cp21778j

cost and provides a framework for further functionalization or decoration. As a gas sorbent, GO is light-weight, highly porous and can be easily chemically modified. Recent experiments revealed that GO composites with MOFs, polyoxometalate nanocomposites, iron and iron oxide, zirconium hydroxide, and aluminium/zirconium–aluminium polyoxycations exhibit promising adsorptive properties for a variety of gases, including NH_3,[33–37] H_2S,[38] SO_2,[39] NO_2,[40] and H_2O.[41] Very recently, graphene oxide frameworks (GOFs) were synthesized and proposed to be a good medium for hydrogen storage at low temperature and CO_2 capture at room temperature.[42] Our first-principles study suggested that titanium-decorated GO (Ti–GO) is able to bind molecular hydrogen strongly at room temperature and is an ideal substrate for hydrogen storage.[43]

Motivated by recent progresses in the GO-based materials, especially the GO composites as gas sorbents, here we proposed Ti-decorated GO as an ideal sorbent for CO separation from gas mixtures, *e.g.*, CO mixed with N_2, CO_2, or CH_4. Our first-principles calculations predicted an appreciable binding energy of $\sim$70 kJ mol^{-1} for CO adsorption on the Ti sites. Grand canonical Monte Carlo (GCMC) simulations of adsorption isotherms further demonstrated the capability of Ti–GO for CO capture and separation with a high capacity and superior selectivity. The present theoretical results not only predict a potential nanomaterial for CO separation, but also give some implications in the applications of GO-based materials for adsorption and capture of selected gases *via* proper metal decoration.

2. Computational methods

The first-principles computations were performed using the density functional theory (DFT) within generalized gradient approximation (GGA) of Perdew, Burke, and Ernzerhof (PBE) parameterization.[44] A projector augmented wave (PAW) method,[45] as implemented in the VASP code,[46] was used to represent the core electrons. The cutoff energy for the plane-wave basis expansion was 500 eV. A periodic supercell was used for modeling the two dimensional GO, where a 3×4 rectangular supercell with 48 C atoms (for Ti–GO motifs) or a $2\sqrt{3} \times \sqrt{3}$ supercell with 12 C atoms (for the periodic Ti–GO model) was used in the GO basal plane and adjacent GO layers were separated by a vacuum region of about 15 Å thickness. The Brillouin zone integration for the 48- and 12-C-atom supercells was done with $3 \times 4 \times 1$ and $4 \times 8 \times 1$ **k** point grids, respectively. All the structures are fully relaxed both in atomic positions and lattice parameters until the forces on atoms are smaller than 0.01 eV Å^{-1}.

To obtain the adsorption isotherms, we performed GCMC simulation[47] with the Dreiding force field.[48] The standard Lennard-Jones (LJ) parameters of the Dreiding force field were used to describe the weak van der Waals (vdW) adsorption of the CO_2 and CH_4 molecules, whereas the LJ parameters for CO and N_2 molecules were elaborately adjusted to reproduce the relatively strong binding energies of these two molecules on the Ti–GO substrates from DFT calculations. GCMC simulations were carried out in the gas pressure range from 0 to 10 bar at room temperature (298 K). In each step of the GCMC simulations, we used one of the four events (insertion, deletion, translation and rotation) on each gas molecule, and computed the energy change. If the energy change was negative, the event was accepted; while if the energy change was positive, then the event was accepted with probability. At each pressure, the GCMC simulation consisted of 1×10^6 steps to allow equilibration, followed by 1×10^7 steps to sample the configuration space.

The Dreiding force field combined with a GCMC technique has been employed before to simulate the gas adsorption behavior of a variety of nanoporous materials.[49,50] In Table S1 of the ESI†, we compare the adsorption energies of these four gaseous molecules on the graphene surface from the Dreiding force field and experiments. These gas–graphene systems are individually optimized with Dreiding force field to find the equilibrium adsorption configuration and to calculate the corresponding adsorption energies. Clearly, the Dreiding force field is able to reproduce the experimental adsorption energies rather well.

It is noteworthy that the Dreiding force field (with either conventional parameters or LJ parameters fitted from the DFT results) were only used in the GCMC simulations in Section 3.3, and the rest of the calculations were all performed by DFT methods. Meanwhile, except that the GCMC simulations are carried on the rigid host lattice, all the structural models are fully optimized using DFT calculations.

3. Results and discussions

3.1 Structural models for Ti-decorated GO

Recently, there have been substantial efforts in searching the stable structural models of GO.[43,51–57] Our previous work has demonstrated that the stable GO phases are composed of some local structural motifs from appropriate combinations of the hydroxyl (**h**) and epoxy (**e**) groups,[51] and certain transition metals, such as Ti, can be strongly anchored by the oxygen-containing groups on the GO surface.[43] These anchored Ti atoms interact strongly with H_2 molecules, making them superior sites for hydrogen adsorption. Recent experiments showed that pristine GO is not a good sorbent for H_2S and SO_2, but the GO composites with $Zr(OH)_4$ or MOFs can be used for gas adsorption with moderate capacity.[38,39] In this work, we started from the stable GO motifs obtained in our previous study[51] and decorated them with Ti atoms aiming to improve the adsorption capability for gas molecules.

We chose two low-energy GO motifs that are composed of two hydroxyl groups and one epoxy group as representative models, labeled as **heh** and **hhe** in Fig. 1a and b, respectively. Fig. 1c and d display the local structural motifs for the Ti-decorated GO, where each Ti atom is attached to two surface oxygen atoms. On these stable GO motifs, the binding energy for the Ti atom is 530 kJ mol^{-1}, which can effectively prevent Ti atoms from clustering on the GO surface.[43] The following studies of gas adsorption are based on these Ti-decorated GO surfaces.

3.2 Gas adsorption on Ti-decorated GO

We studied the adsorption of four typical gases, namely, CO, N_2, CO_2 and CH_4, on the Ti-decorated GO. Table 1 summarizes the adsorption energies and distances between gas molecules and

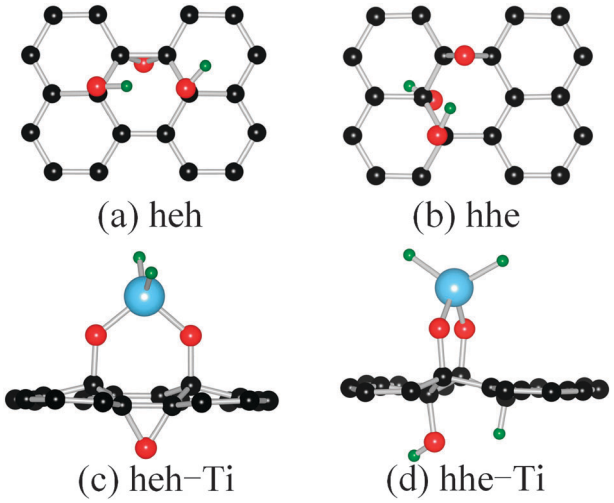

Fig. 1 Structural models for representative GO motifs of (a) **heh** and (b) **hhe**, and those decorated with Ti atoms: (c) Ti–**heh** and (d) Ti–**hhe**. Black balls denote carbon atoms, red balls for oxygen atoms, green balls for hydrogen atoms, and light blue balls for Ti atoms.

Table 1 Adsorption energies E_{ads} (kJ mol^{-1}) and distances d_{Ti-gas} (Å) for the gases (CO, N_2, CO_2 and CH_4) adsorbed on different GO structures. The adsorption energies for periodic model denote adsorption of the first molecule

	heh motif		**hhe** motif		Periodic model	
Gas	E_{ads}/ kJ mol^{-1}	d_{Ti-gas}/Å	E_{ads}/ kJ mol^{-1}	d_{Ti-gas}/Å	E_{ads}/ kJ mol^{-1}	d_{Ti-gas}/Å
CO	67.6	2.15	67.0	2.17	71.5	2.14
N_2	19.3	2.23	19.6	2.24	20.1	2.22
CO_2	3.9	3.41	3.2	3.55	4.2	3.58
CH_4	1.6	4.30	1.8	4.11	2.3	4.02

Ti atom on the GO surface with different local structures. First, these two structural motifs yield nearly identical adsorption energies and molecule–Ti distances, suggesting that the gas adsorption behaviors are not sensitive to the local structures of GO as long as the Ti atoms are strongly anchored on the surface. Among the four gases studied, CO has the strongest adsorption energies ($\sim$70 kJ mol^{-1}) on Ti. The adsorption energies of N_2 are $\sim$20 kJ mol^{-1}, which are also higher than the strength of typical vdW interaction. Accordingly, the distances between the CO/N_2 molecules and Ti atoms are within 2.3 Å. On the contrary, for the CO_2 and CH_4 molecules, the adsorption strengths are less than 5 kJ mol^{-1} with the adsorption distances of 3–4 Å, suggesting a typical vdW interaction. The present DFT results clearly indicate that Ti has a strong capability to adsorb CO molecules preferentially and the Ti-decorated GO materials might be used for CO capture and separation.

The adsorption strengths of CO on the Ti-decorated GO from present GGA-PBE calculations fall in the range of the interaction energies between CO and other sorbents in previous studies, for example, 163 kJ mol^{-1} calculated at the BLYP/VD(T)ZP level and 151 kJ mol^{-1} measured by experiments for the CO molecule adsorbed on the Cu^+ sites in the high-silica zeolites,[58] 122 kJ mol^{-1} between CO and the acid sites in zeolites at the MP2 computational level,[59] a maximum value of 70 kJ mol^{-1} for CO adsorbed on zeolite 5A and 13X from

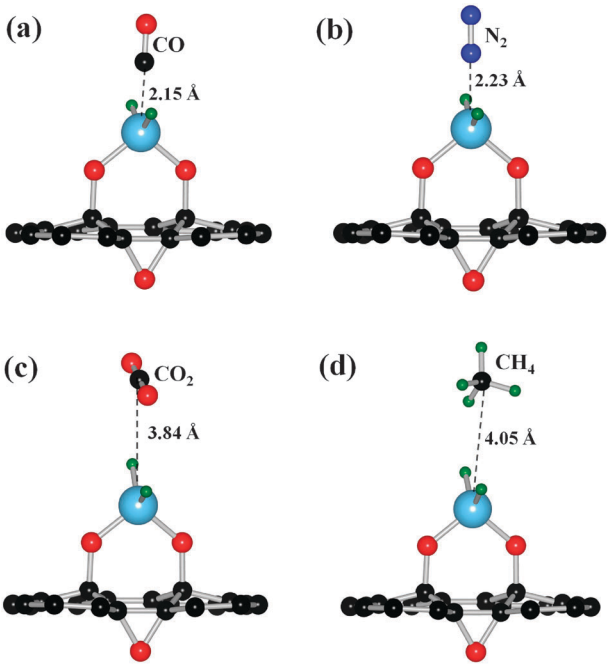

Fig. 2 Optimized structures of the gases (CO, N_2, CO_2 and CH_4) adsorbed on the Ti-decorated GO motif (Ti–**heh**). Nitrogen atoms are represented by blue balls, while the coloring scheme for other atoms is the same as in Fig. 1.

experimental heat of adsorption,[10] $\sim$20 kJ mol^{-1} for CO adsorbed on MOF-5 and MOF-177 in experiments.[10]

When a single CO or N_2 molecule is adsorbed on the Ti-decorated GO surface, the molecule adopts a head-on configuration and forms linear complexes with Ti (see Fig. 2a and b). Though CO and N_2 molecules have relatively strong binding energies with Ti, their adsorptions do not induce noticeable structural changes on the Ti–GO substrate. After adsorption, the equilibrium C–O and N–N bond lengths in these two molecules are 1.151 Å and 1.119 Å, respectively, which are slightly longer than the bond lengths of isolated CO and N_2 molecules (1.143 Å and 1.113 Å). Different from the cases of CO and N_2, the CO_2 molecule adopts a tilted configuration on Ti (Fig. 2c), with a Ti–CO_2 distance of 3.41 Å and a Ti–O–C angle of 102°, similar to the case of CO_2 adsorption on the Mg-MOF-74 surface.[23] The binding energy of CO_2 on Ti is $\sim$4 kJ mol^{-1}. CH_4 has an even lower binding energy of only $\sim$2 kJ mol^{-1} and the Ti–CH_4 distance is 4.30 Å (Fig. 2d). It is worthy to point out that the DFT/GGA methodology is usually insufficient for describing the weak van der Waals (dispersion) interaction and thus the adsorption energies for CO_2 and CH_4 from DFT calculations are not very accurate. However, the present DFT calculations are still qualitatively correct in predicting the relative strengths of molecule–substrate interaction, that is, adsorption energies of CO_2 and CH_4 on a Ti–GO sorbent are weaker and those for N_2 and CO are much stronger, which is important to discuss the following gas separation properties.

We further considered the gas adsorption on a GO substrate with densely distributed Ti atoms using a periodic GO model (Fig. 3a). This model was originally proposed for studying the hydrogen storage property of GO[43] and was shown to reproduce

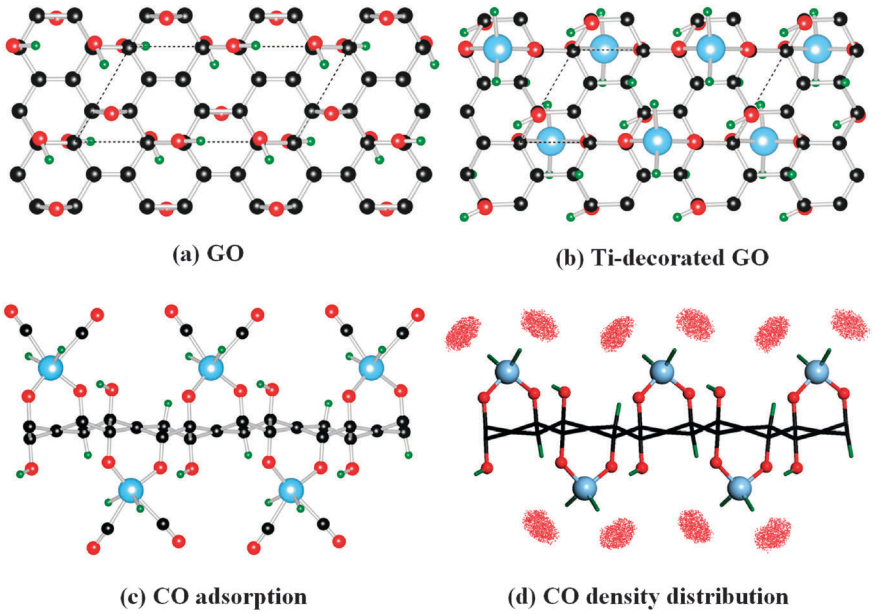

Fig. 3 (a) Periodic GO model used in this work; (b) Ti decorated on both sides of GO surface; (c) Ti-decorated GO with fully loaded CO molecules; (d) density distribution for CO molecules on the Ti-decorated GO at 298 K and 10 bar from GCMC simulation. The red points are the centers-of-mass of the adsorbed CO molecules (each point denotes one CO molecule).

the experimental NMR data quite well.[56] The C/O ratio in this GO model is 2 : 1, which falls in the experimental range of 1.8–2.5.[57] Following our previous work,[43] this GO model was further stabilized by hydrogenation and then decorated by Ti with a concentration of one Ti per six C atoms. The optimized structure of a Ti-decorated GO model is depicted in Fig. 3b. After hydrogenation, Ti can be dispersed on both sides of the GO surface. Each Ti atom is strongly anchored by two oxygen atoms with a large binding energy of 476 kJ mol^{-1}.

On the periodic model of Ti-decorated GO (Fig. 3b), the gas adsorption properties including adsorption energies and molecule–Ti distances are similar to the above results on Ti-decorated GO motifs (see Table 1). The adsorption energies of the four gases (CO, N_2, CO_2 and CH_4) on the periodic Ti–GO model are all slightly stronger than those on the isolated GO motifs. For CO adsorption, Fig. 3c shows the Ti-decorated GO fully loaded with CO molecules on both sides of a monolayer sheet, and each Ti can bind two CO molecules with an adsorption energy of 71 kJ mol^{-1} for the first one and 33 kJ mol^{-1} for the second one. The N_2 adsorption energy is 20 kJ mol^{-1} with an N_2–Ti distance of 2.22 Å. For CO_2 and CH_4, the adsorption energies are 4.2 kJ mol^{-1} and 2.3 kJ mol^{-1}, respectively, which are also consistent with the results on isolated GO motifs.

To gain deeper insight into the interaction between gas molecules and the GO sorbents, we analyze the local electronic density of states (LDOS) for the d component of Ti and the s and p components of gas molecules, which are displayed in Fig. 4. The Ti-decorated GO substrate is described by the model in Fig. 3b. When a CO or a N_2 molecule is adsorbed on the Ti site, a molecular orbital emerges in the conduction band. This orbital induce the hybridization between an empty d orbital of Ti and an occupied p orbital of the CO/N_2 molecule, indicating a dative bonding.[60] On the contrary, in

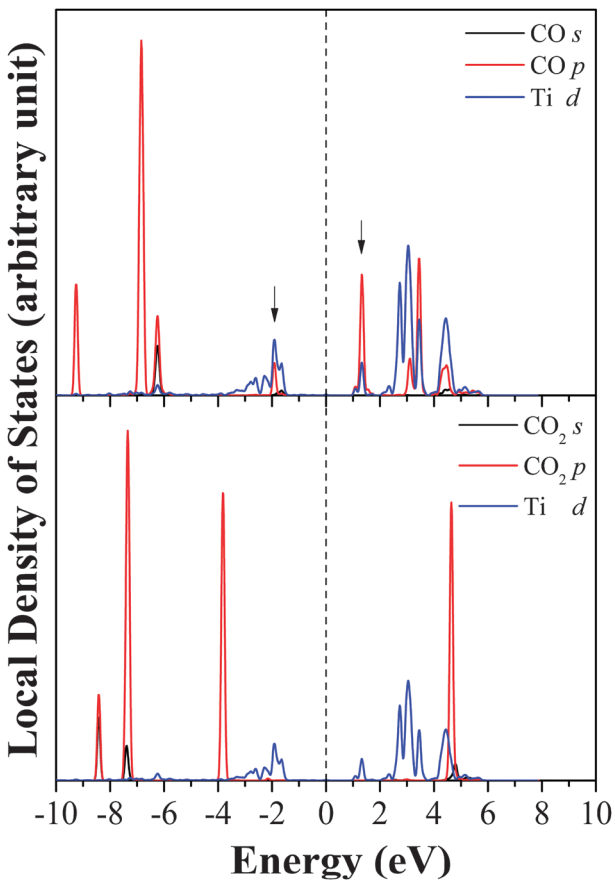

Fig. 4 Local density of states (LDOS) for the d component of Ti and the s and p components of gas molecules (CO and CO_2) in the Ti decorated GO model (Fig. 3b). The dashed lines indicate the Fermi level defined by the top of valence band; the arrows mark the hybridization orbitals between Ti and CO molecules.

the case of CO_2/CH_4 adsorption, such p–d hybridization is absent. This suggests that the strong adsorption energies in the case of CO and N_2 at the Ti sites originate from the p–d hybridization.

3.3 Gas adsorption isotherms

GCMC simulations were performed to further verify the adsorption properties of CO, N_2, CO_2 and CH_4 at room temperature (298 K). The adsorption isotherms for each of these four gases on the periodic model of Ti-decorated GO are shown in Fig. 5a. One can see that the amounts of gas adsorption increase with increasing pressure over the entire pressure range studied (from 0 to 10 bar). Only the CO adsorption gradually approaches saturation, which indicates a stronger adsorption strength.[10] The Ti-decorated GO sorbent presents the largest adsorption capacity for CO and the amount reaches 7.5 mmol g^{-1} under the pressure of 10 bar at 298 K. At the pressure of 1 bar, the adsorption amount is 4.9 mmol g^{-1}, which is significantly higher than the amounts of CO adsorption on zeolites and MOFs (less than 2 mmol g^{-1}) measured under the same pressure/temperature conditions.[8,10]

According to GCMC simulation, up to the pressure of 10 bar, each Ti uptakes about 1.3 CO molecules on average, a little lower than the first-principles prediction that each Ti atom can interact strongly with two CO molecules with an average binding energy of ~52 kJ mol^{-1}. This difference can be partially attributed to the temperature effect, that is, the adsorption amount increases as the temperature decreases. To understand this, we simulated the CO adsorption at a low temperature of 200 K (under the same pressure of 10 bar) and the average CO uptake increases to ~1.9 molecules per Ti, which is closer to two molecules per Ti by first-principles calculations.

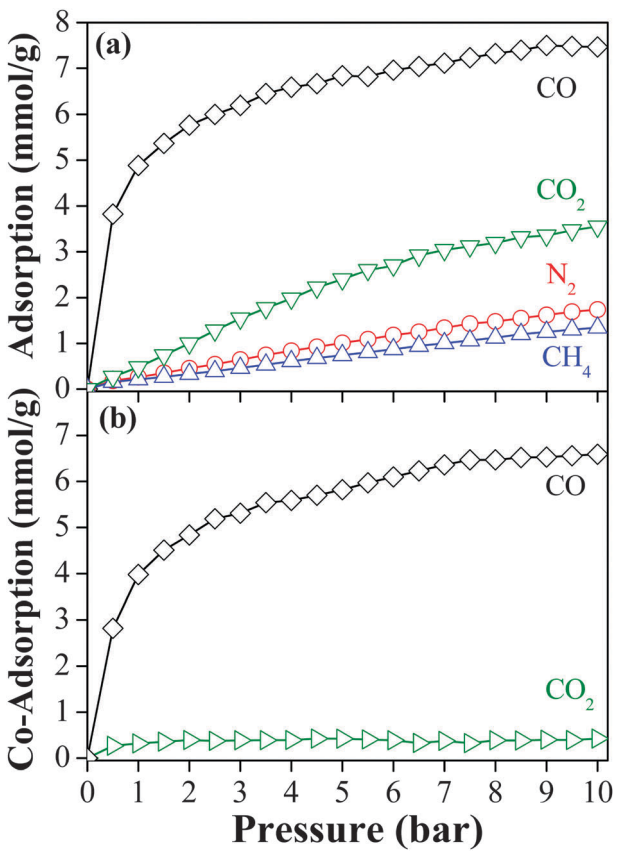

Fig. 5 (a) Adsorption isotherms of different gases (CO, N_2, CO_2 and CH_4) adsorbed individually on the Ti-decorated GO surface at 298 K; (b) co-adsorption isotherms of CO/CO_2 gas mixture at 298 K.

The density distribution of the CO molecules adsorbed on the Ti-decorated GO at the pressure of 10 bar is shown in Fig. 3d. The CO molecules do not distribute uniformly, but congregate around the Ti sites, which is consistent with our static first-principles calculations of CO adsorption (Fig. 3c). Compared with CO, other gases like N_2, CO_2, and CH_4 exhibit relatively smaller adsorption amounts due to the weaker binding energies, suggesting the Ti-decorated GO is a potential sorbent for separating CO from mixtures with other gases. As can be seen in Fig. 5a, CO_2 exhibits an intermediate adsorption amount though it has weak interaction with Ti. This is due to the relatively strong interaction between CO_2 and graphene described by the Dreiding Force Field (see Table S1 of the ESI†). Accordingly, the CO_2 molecules mostly distribute on the GO surface instead of the vicinity of Ti atoms (see Fig. S1 of the ESI†).

The capability of CO capture and separation is further confirmed by the GCMC simulation of co-adsorption of CO with the other gases. As an example, Fig. 5b shows the co-adsorption isotherm of a CO/CO_2 gas mixture. The adsorption amounts of both CO and CO_2 decrease with regard to the individual adsorption, for example, at 10 bar the CO adsorption slightly reduces from 7.5 to 6.6 mmol g^{-1}, while the CO_2 uptake becomes very little. We speculate that the main reason for the amount reduction in co-adsorption is the repulsive interaction between different gas molecules, namely, the steric exclusion effect. This effect is also consistent with the previous experimental observation in the CO_2 separation from N_2/CH_4 gas mixtures, where the amounts of co-adsorption are lower than those of individual adsorptions.[25] Similar preferential CO adsorption is also found in the CO/N_2 and CO/CH_4 gas mixtures (see Fig. S2 of the ESI†), which makes the Ti-decorated GO material highly attractive and potential for CO separation from these gas mixtures. Moreover, by carefully choosing and decorating different metals on the GO substrates, selective adsorption of other gas molecules on the GO substrate could be realized. For instance, our preliminary calculations show that magnesium atoms supported on the GO surface can interact strongly with CO_2 molecules. Designing novel metal-decorated graphene oxide materials as the ideal sorbents for capture/separation of different gases is still under way.

4. Conclusions

The adsorption properties of selected gases (CO, N_2, CO_2 and CH_4) on the Ti-decorated GO surface have been systematically studied by first-principles calculations and GCMC simulations. Among the four gases studied, large adsorption energy (~70 kJ mol^{-1}) is found for CO molecules on Ti sites, which is not sensitive to the local structures of the GO substrate. Such a strong interaction can be attributed to the

p–d hybridization between CO molecule and Ti. GCMC simulations of adsorption isotherms further demonstrate that the adsorption amount of CO gas can reach as high as 7.5 mmol g^{-1} at 10 bar and room temperature, and the selective adsorption of CO from gas mixtures can be achieved. Our results show that the Ti-decorated GO materials can be ideal sorbents for CO capture and separation from mixtures with N_2, CO_2, and CH_4. In addition to Ti, GO-based materials with other metal decoration may find potential applications for capture and separation of other gases.

Acknowledgements

The work in China was supported by the Fundamental Research Funds for the Central Universities of China (No. DUT10ZD211) and National Natural Science Foundation of China (40874039, 20873068, 11134005). The work in the US was supported by the US Department of Energy under Grant No. DE-SC0002623.

References

1 J. A. Raub, M. Mathieu-Nolf, N. B. Hampson and S. R. Thom, *Toxicology*, 2000, **145**, 1–14.
2 B. C. H. Steele and A. Heinzel, *Nature*, 2001, **414**, 345–352.
3 E. D. Park, D. Lee and H. C. Lee, *Catal. Today*, 2009, **139**, 280–290.
4 A. Tanksale, J. N. Beltramini and G. M. Lu, *Renewable Sustainable Energy Rev.*, 2010, **14**, 166–182.
5 G. Sethia, G. P. Dangi, A. L. Jetwani, R. S. Somani, H. C. Bajaj and R. V. Jasra, *Sep. Sci. Technol.*, 2010, **45**, 413–420.
6 M. W. Ackley, S. U. Rege and H. Saxena, *Microporous Mesoporous Mater.*, 2003, **61**, 25–42.
7 Y. Xie, J. Zhang, J. Qiu, X. Tong, J. Fu, G. Yang, H. Yan and Y. Tang, *Adsorption*, 1997, **3**, 27–32.
8 R. S. Pillai, G. Sethia and R. V. Jasra, *Ind. Eng. Chem. Res.*, 2010, **49**, 5816–5825.
9 Y.-Y. Huang, *J. Catal.*, 1973, **30**, 187–194.
10 D. Saha and S. Deng, *J. Chem. Eng. Data*, 2009, **54**, 2245–2250.
11 T. Montanari, I. Salla and G. Busca, *Microporous Mesoporous Mater.*, 2008, **109**, 216–222.
12 S. Sircar, T. C. Golden and M. B. Rao, *Carbon*, 1996, **34**, 1–12.
13 H. Tamon, K. Kitamura and M. Okazaki, *AIChE J.*, 1996, **42**, 422–430.
14 S. E. Iyuke, A. B. Mohamad, W. R. Daud, A. A. Kadhum, Z. Fisal and A. M. Shariff, *J. Chem. Technol. Biotechnol.*, 2000, **75**, 803–811.
15 C. A. Grande, F. V. S. Lopes, A. M. Ribeiro, J. M. Loureiro and A. E. Rodrigues, *Sep. Sci. Technol.*, 2008, **43**, 1338–1364.
16 A. B. Mohamad, S. E. Iyuke, W. R. W. Daud, A. A. H. Kadhum, Z. Fisal, M. F. Al-Khatib and A. M. Shariff, *J. Mol. Struct.*, 2000, **550–551**, 511–519.
17 R. W. Triebe and F. H. Tezel, *Gas Sep. Purif.*, 1995, **9**, 223–230.
18 L. Predescu, F. Tezel and S. Chopra, *Adsorption*, 1997, **3**, 7–25.
19 Q. Min Wang, D. Shen, M. Bulow, M. Ling Lau, S. Deng, F. R. Fitch, N. O. Lemcoff and J. Semanscin, *Microporous Mesoporous Mater.*, 2002, **55**, 217–230.
20 D. Britt, D. Tranchemontagne and O. M. Yaghi, *Proc. Natl. Acad. Sci. U. S. A.*, 2008, **105**, 11623–11627.
21 J.-R. Li, R. J. Kuppler and H.-C. Zhou, *Chem. Soc. Rev.*, 2009, **38**, 1477–1504.
22 R. Zou, A. I. Abdel-Fattah, H. Xu, Y. Zhao and D. D. Hickmott, *CrystEngComm*, 2010, **12**, 1337–1353.
23 L. Valenzano, B. Civalleri, S. Chavan, G. T. Palomino, C. O. Arean and S. Bordiga, *J. Phys. Chem. C*, 2010, **114**, 11185–11191.
24 J. W. Yoon, Y.-K. Seo, Y. K. Hwang, J.-S. Chang, H. Leclerc, S. Wuttke, P. Bazin, A. Vimont, M. Daturi, E. Bloch, P. L. Llewellyn, C. Serre, P. Horcajada, J.-M. Grenèche, A. E. Rodrigues and G. Férey, *Angew. Chem., Int. Ed.*, 2010, **49**, 5949–5952.
25 M. Radha Kishan, J. Tian, P. K. Thallapally, C. A. Fernandez, S. J. Dalgarno, J. E. Warren, B. P. McGrail and J. L. Atwood, *Chem. Commun.*, 2010, **46**, 538–540.
26 R. Banerjee, H. Furukawa, D. Britt, C. Knobler, M. O'Keeffe and O. M. Yaghi, *J. Am. Chem. Soc.*, 2009, **131**, 3875–3877.
27 S. R. Venna and M. A. Carreon, *J. Am. Chem. Soc.*, 2009, **132**, 76–78.
28 A. K. Geim, *Science*, 2009, **324**, 1530–1534.
29 A. K. Geim and K. S. Novoselov, *Nat. Mater.*, 2007, **6**, 183–191.
30 D. R. Dreyer, S. Park, C. W. Bielawski and R. S. Ruoff, *Chem. Soc. Rev.*, 2010, **39**, 228–240.
31 Z. Wei, D. Wang, S. Kim, S.-Y. Kim, Y. Hu, M. K. Yakes, A. R. Laracuente, Z. Dai, S. R. Marder, C. Berger, W. P. King, W. A. de Heer, P. E. Sheehan and E. Riedo, *Science*, 2010, **328**, 1373–1376.
32 Y. Zhu, S. Murali, W. Cai, X. Li, J. W. Suk, J. R. Potts and R. S. Ruoff, *Adv. Mater.*, 2010, **22**, 3906–3924.
33 M. Seredych and T. J. Bandosz, *J. Colloid Interface Sci.*, 2008, **324**, 25–35.
34 C. Petit and T. J. Bandosz, *J. Mater. Chem.*, 2009, **19**, 6521–6528.
35 C. Petit and T. J. Bandosz, *J. Phys. Chem. C*, 2009, **113**, 3800–3809.
36 C. Petit, B. Mendoza and T. J. Bandosz, *Langmuir*, 2010, **26**, 15302–15309.
37 C. Petit and T. J. Bandosz, *Adv. Funct. Mater.*, 2010, **20**, 111–118.
38 C. Petit, B. Mendoza and T. J. Bandosz, *ChemPhysChem*, 2010, **11**, 3678–3684.
39 M. Seredych and T. J. Bandosz, *J. Phys. Chem. C*, 2010, **114**, 14552–14560.
40 S. Bashkova and T. J. Bandosz, *Ind. Eng. Chem. Res.*, 2009, **48**, 10884–10891.
41 K. Morishige and T. Hamada, *Langmuir*, 2005, **21**, 6277–6281.
42 J. W. Burress, S. Gadipelli, J. Ford, J. M. Simmons, W. Zhou and T. Yildirim, *Angew. Chem., Int. Ed.*, 2010, **49**, 8902–8904.
43 L. Wang, K. Lee, Y.-Y. Sun, M. Lucking, Z. Chen, J. J. Zhao and S. B. Zhang, *ACS Nano*, 2009, **3**, 2995–3000.
44 J. P. Perdew, K. Burke and M. Ernzerhof, *Phys. Rev. Lett.*, 1996, **77**, 3865.
45 G. Kresse and D. Joubert, *Phys. Rev. B: Condens. Matter*, 1999, **59**, 1758.
46 G. Kresse and J. Furthmüller, *Phys. Rev. B: Condens. Matter*, 1996, **54**, 11169.
47 D. Frenkel and B. Smit, *Understanding Molecular Simulations: From Algorithms to Applications*, 2nd edn, Academic Press, San Diego, 2002.
48 S. L. Mayo, B. D. Olafson and W. A. Goddard, *J. Phys. Chem.*, 1990, **94**, 8897–8909.
49 J. Liu, J. Y. Lee, L. Pan, R. T. Obermyer, S. Simizu, B. Zande, J. Li, S. G. Sankar and J. K. Johnson, *J. Phys. Chem. C*, 2008, **112**, 2911–2917.
50 G. Garberoglio, A. I. Skoulidas and J. K. Johnson, *J. Phys. Chem. B*, 2005, **109**, 13094–13103.
51 L. Wang, Y. Y. Sun, K. Lee, D. West, Z. F. Chen, J. J. Zhao and S. B. Zhang, *Phys. Rev. B: Condens. Matter*, 2010, **82**, 161406.
52 H. J. Xiang, S.-H. Wei and X. G. Gong, *Phys. Rev. B: Condens. Matter*, 2010, **82**, 035416.
53 J.-A. Yan, L. Xian and M. Y. Chou, *Phys. Rev. Lett.*, 2009, **103**, 086802.
54 D. W. Boukhvalov and M. I. Katsnelson, *J. Am. Chem. Soc.*, 2008, **130**, 10697–10701.
55 R. J. W. E. Lahaye, H. K. Jeong, C. Y. Park and Y. H. Lee, *Phys. Rev. B: Condens. Matter*, 2009, **79**, 125435.
56 N. Lu, Y. Huang, H.-b. Li, Z. Li and J. Yang, *J. Chem. Phys.*, 2010, **133**, 034502–034507.
57 T. Szabo, O. Berkesi, P. Forgo, K. Josepovits, Y. Sanakis, D. Petridis and I. Dekany, *Chem. Mater.*, 2006, **18**, 2740–2749.
58 M. Davidova, D. Nachtigallova, R. Bulanek and P. Nachtigall, *J. Phys. Chem. B*, 2003, **107**, 2327–2332.
59 S. Bates and J. Dwyer, *J. Phys. Chem.*, 1993, **97**, 5897–5900.
60 Y. Y. Sun, Y.-H. Kim, K. Lee, D. West and S. B. Zhang, *Phys. Chem. Chem. Phys.*, 2011, **13**, 5042–5046.